

Advances in AFM: Seeing Atoms in Ambient Conditions*

Alfred J. Weymouth,[†] Daniel Wastl, and Franz J. Giessibl*Department of Physics, University of Regensburg,
Universitaetsstrasse 31, 93053 Regensburg, Germany*

(Received 5 February 2018; Accepted 14 July 2018; Published 2 August 2018)

It's hard to imagine that we can take a splinter and sharpen it down to the atomic level. It's even more impressive that we can bring this sharp tip close to a surface, scan it over the surface, and be sensitive to the tiny forces between the apex atom and individual atoms on the surface. Measuring and interpreting these forces is the goal of high-resolution atomic force microscopy (AFM). We perform frequency-modulation AFM (FM-AFM), in which we oscillate the tip and record the change in frequency as a measure of the interaction with the surface. FM-AFM performed in vacuum with stiff sensors has led to amazing discoveries. Now, we are returning to the challenge of imaging samples in device- and biologically-relevant conditions. This contribution summarizes work that was performed in the Giessibl group to image with atomic resolution in ambient and liquid environments. We demonstrated atomic resolution with the qPlus sensor on KBr, and followed this with investigations on graphitic surfaces. We have also shown single-atomic defects and steps on the calcite surface. [DOI: 10.1380/ejsnt.2018.351]

Keywords: Atomic force microscopy; Solid-liquid interfaces; Water

I. INTRODUCTION

Atomic force microscopy (AFM) is a unique tool for investigating surfaces and adsorbates at the atomic scale. A probe ending in a sharp tip is moved across a surface to determine properties of the sample close to the tip apex. When the tip is close enough to the surface, it can be sensitive to individual atoms [1]. Investigating samples locally is very different from the majority of techniques used to probe samples at the atomic scale. Most require a (relatively) large sample to be irradiated. AFM is capable of atomic resolution in ambient conditions, does not require a conductive substrate, and there are exciting applications in many fields including semiconductor devices and medical biophysics. More specifically, non-contact AFM could hold the key to characterizing biological samples at the atomic scale.

AFM in ambient conditions is typically performed in amplitude-modulation mode [2]. The cantilever is excited at a fixed frequency and its amplitude changes as the tip and surface interact. This method is typically not a true non-contact method, but rather intermediate contact, as the tip “touches” the surface with each oscillation cycle. AFM can also be performed in a true non-contact mode (similar to the scanning tunneling microscope). In 1993, Ohnesorge and Binnig reported true atomic resolution with AFM in static mode (without an oscillating cantilever) on the calcite surface [3]. In 2005, Fukuma, Kobayashi, Matsushige, and Yamada demonstrated atomic-scale imaging with non-contact AFM in liquid with a relatively soft cantilever ($k = 42 \text{ N/m}$) [4].

We conduct measurements with qPlus AFM sensors operating in a non-contact mode [5]. At low-temperature and in UHV, the qPlus has been used to image single molecular adsorbates and small metal clusters with unprecedented spatial resolution [6, 7]. Our aim is to pur-

sue high-resolution AFM imaging with the qPlus sensor in device- and biologically-relevant conditions.

In 2012, Ichii and co-workers demonstrated that the qPlus could achieve atomic resolution in ionic liquids [8]. This paper summarizes three important steps we took pursuing imaging with high spatial resolution outside of vacuum. When we were first able to achieve atomic resolution, we realized that small amplitudes of oscillation were important for a high signal-to-noise ratio, which we understood because of the influence of water layers, as sketched in Fig. 1 [9]. A second step was the demonstration of the influence that bulk tip material had upon tip-sample interaction. Because the water layer plays such a large role, there are strong differences in acquiring data with a hydrophilic versus a hydrophobic tip [10]. Finally, we could show observations of a single-atom defect and an atomic step with atomic resolution on either terrace [11].

II. EXPERIMENTAL METHOD

Frequency-modulation AFM is a technique in which the cantilever is oscillated at its resonance frequency and the change of frequency is a measure of the tip-sample interaction, as illustrated in Fig. 2 [12]. For small amplitudes, the cantilever acts as a spring with linear spring constant

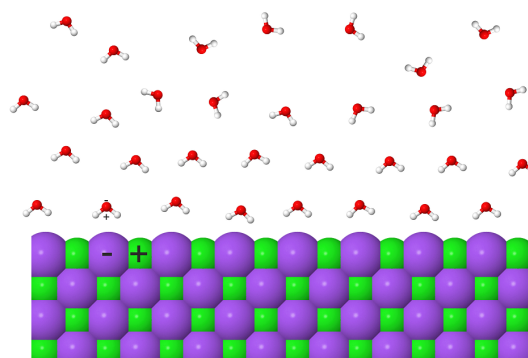


FIG. 1. A hydration layer naturally forms on many surfaces in ambient conditions. On the polar KBr surface, the closest molecules order, and this order is weaker the further the molecules are from the surface.

* This paper was presented as the award lecture for the Heinrich Rohrer Medal –Rising Medal– at the 8th International Symposium on Surface Science, Tsukuba International Congress Center, Tsukuba, Japan, October 22-26, 2017.

[†] Corresponding author: jay.weymouth@ur.de

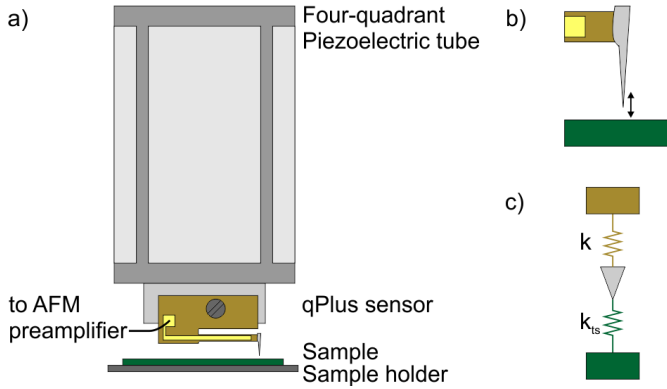


FIG. 2. (a) Experimental setup. (b) The tip is oscillated above the surface. (c) The interaction between tip and sample can be thought of as adding another spring, k_{ts} , to a damped driven harmonic oscillator.

k having an effective mass m . The interaction between the tip and the sample can be expressed in terms of the derivative of the force F_{ts} , the force gradient $k_{ts} = -dF_{ts}/dz$. If k_{ts} is constant over an oscillation amplitude, then the resonance frequency shifts by

$$\Delta f = \frac{f_0}{2k} k_{ts}. \quad (1)$$

qPlus sensors are much stiffer than conventional cantilevers, with stiffnesses around $k \approx 2000$ N/m and a free resonance frequency $f_0 \approx 30$ kHz. The oscillation is electrically detected via a preamplifier. As the field continues to advance, recent work has shown that with a state-of-the-art preamplifier, the achievable deflection noise density can be decreased to $n_q = 28$ fm/ $\sqrt{\text{Hz}}$ [13].

As a driven cantilever acts as a damped driven harmonic oscillator, its damping can be expressed by the quality factor, Q . The Q factor describes the energy loss per cycle, ΔE , as a function of the total energy stored in the oscillator, $E = \frac{1}{2}kA^2$, where A is the amplitude of oscillation:

$$Q = 2\pi \frac{E}{\Delta E} \quad (2)$$

The Q factor is an important term in FM-AFM as it is one of the key parameters in the noise terms of FM-AFM measurements [12].

The two dominant noise terms in our setup come from thermal excitation of the cantilever and detection of the frequency. Both strongly depend upon the bandwidth at which data is collected, B . Expressed as the lowest detectable force gradient [14], thermal noise limits us to

$$k_{ts,th} = \sqrt{\frac{4k k_B T B}{\pi f_0 A^2 Q}} \quad (3)$$

Detector noise limits us to

$$k_{ts,det} = \sqrt{\frac{8k n_q B^{3/2}}{3 f_0 A}} \quad (4)$$

All experimental results reported here were carried out at room temperature (approximately 21°C) and at approximately 40–60% relative humidity. At these con-

ditions, capillary condensation is expected (see, e.g., Ref. [15]). When the tip is close to the surface, the additional van der Waals attraction from the tip and surface encourage condensation of water that is present in the air. This capillary condensation produces a relatively large water layer where the tip is present.

III. ADVANTAGES OF SMALL AMPLITUDES

The work discussed in this section has been previously reported in Ref. [9].

We were first able to achieve atomic resolution outside of vacuum of the KBr surface. KBr has a rock salt structure and presents a square lattice along the (100) plane. The crystal was cleaved with a razor blade and mounted to a sample holder.

After approaching the surface, we observed step motion, which has been previously observed on the KBr surface and previously attributed to dissolution in the water layer [16]. A clear observation of this water layer is shown in the $\Delta f(z)$ spectrum, shown in Fig. 3. Data is compared between a surface that has been left for hours in ambient conditions, in Fig. 3(a), and one that was dried with a heat gun, in Fig. 3(b). In Fig. 3(a), there are several abrupt steps in the Δf signal, which we attribute to breaking or rearrangement of the water layers as the tip pulls out of them. When the surface is dried, only one step can be seen. There is also a large difference in the drive signal. With the tip close to the surface, the drive signal differs between wet and dry surfaces by an order of magnitude. This is a signature of the strong damping effect that the water has on the cantilever oscillation.

Assuming that the damping was primarily coming from hydrodynamic forces, we wanted to characterize it as a

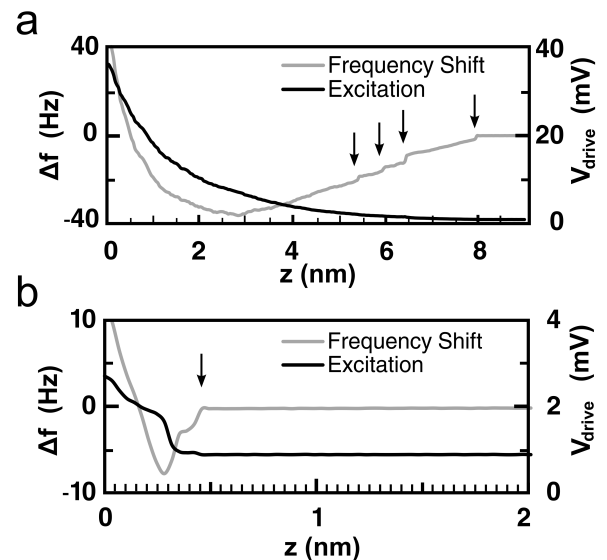


FIG. 3. (a) z -spectrum of Δf and the drive signal over a sample in ambient conditions. The tip was then retracted and the sample dried with a heat gun. (b) z -spectrum immediately following drying. The vertical arrows indicate a signature of water layers. Reprinted with permission from Wastl *et al.*, Phys. Rev. B **87**, 245415 (2013) [9]. Copyright 2013 American Physical Society.

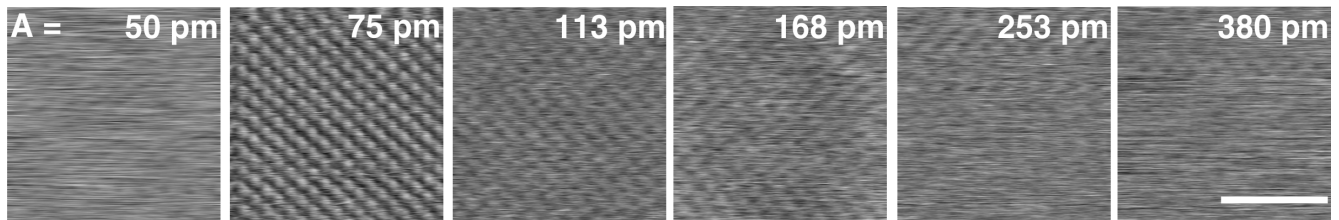


FIG. 4. Amplitude dependence above the KBr surface. Amplitudes are shown in each frame. Images are shown without filtering. Data were lined flattened. The scale bar, the same length for all images, corresponds to 3 nm. Reprinted with permission from Wastl *et al.*, Phys. Rev. B **87**, 245415 (2013) [9]. Copyright 2013 American Physical Society.

function of the amplitude of oscillation. We could then use it, along with a model of the measured signal, to determine the amplitude which maximized the signal-to-noise ratio for our measurements.

Another way of describing the damping from the water is via the quality factor of the oscillator. In vacuum, Q describes the damping of the cantilever. The natural extension is to include hydrodynamic damping in Q when the tip is partially immersed in a liquid layer. The importance of damping to AFM operation can be appreciated by noting that Q is present in both the thermal and oscillator noise terms. In order to characterize Q with the tip near the surface, we measured the excitation of the sensor both close to the surface and far from the surface as a function of the amplitude. We calculated the additional energy loss caused by the liquid layer [17], and expressed this as an overall quality factor. Over the KBr surface, Q had a local maximum at amplitudes slightly less than $A = 100$ pm. Using this $Q(A)$ plot, we calculated the resulting noise.

Following the procedure given by Giessibl in Ref. [18], we estimated the signal term as a decaying exponential keeping the closest point of approach of the tip constant. Previous work proposed that the decay length of the tip-sample interaction with an ionic crystal can be estimated using the lattice constant a_0 by $\lambda = \frac{a_0}{2\sqrt{2}\pi}$ [19]. This description does not include the screening effect of water molecules, meaning it overestimates the signal at greater tip-sample distances. The highest signal-to-noise ratio for this system was predicted to be achieved with an amplitude just under $A = 100$ pm.

We took images at a range of amplitudes, shown in Fig. 4. The highest quality image was observed at an amplitude of $A = 75$ pm.

Already in 1983 it was experimentally demonstrated by Israelachvili and Pashley that water orders in layers on a surface [20]. On a mica surface, water layers are spaced by 250 pm [20]. At an amplitude of 75 pm, and a peak-to-peak amplitude of 150 pm, we propose that the tip is oscillating within a single water layer above the KBr surface. The energy cost of leaving and re-penetrating a water layer has a direct impact on the noise terms, which can be minimized when oscillating with small amplitudes.

IV. IMPORTANCE OF THE TIP MATERIAL

The work discussed in this section was first reported in Ref. [10].

One advantage of the qPlus sensor is that any tip ma-

terial can be glued to the cantilever. Our group typically uses tungsten as a tip material because there are many known etching procedures, which we have found to be reliable in creating a sharp tip. When probing an insulating surface, we do not require a conductive tip, which means many more materials are suitable as tip materials. Silicon oxidizes easily in air and the resulting oxide is naturally hydrophilic, due to the oxide groups. Silicon is a brittle crystal and splinters easily. Small, sharp splinters which are suitable for tips can easily be made. Sapphire is another hard material and unlike silicon, is hydrophobic [22].

We investigated graphene with both silicon and sapphire tips. The sample was hydrogen-intercalated graphene grown on 6H-SiC(0001) [23]. We obtained atomic resolution with both tip materials, and collected $\Delta f(z)$ spectra from the imaging distance away from the surface, until we could no longer detect interaction, shown in Fig. 5. With the hydrophilic silicon tip, the $\Delta f(z)$ curve showed measurable interaction over 100 nm from the imaging distance. In contrast, with the hydrophobic sapphire tip, we recorded interaction only 15 nm from the surface.

We found that sapphire tips can be produced much sharper compared to the bulk-Si tips, but it is more difficult to achieve atomic resolution on graphene with them.

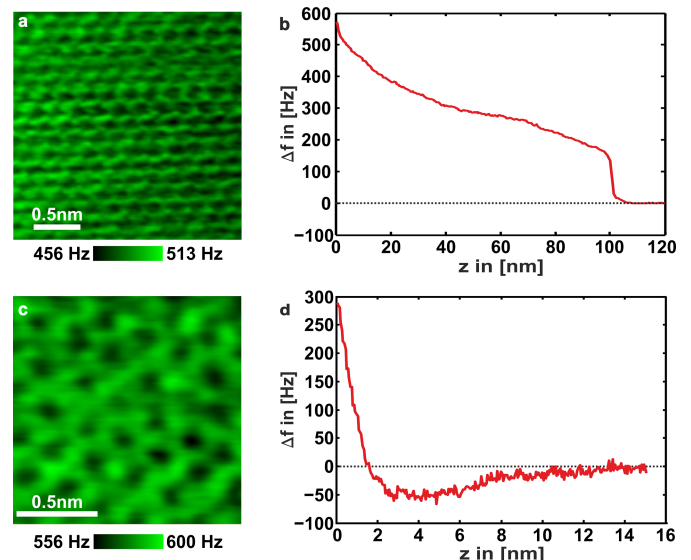


FIG. 5. Measurements on graphene. (a) Atomic resolution with a bulk-Si tip. (b) Corresponding $\Delta f(z)$ spectrum. (c) Atomic resolution with a sapphire tip. (d) Corresponding $\Delta f(z)$ spectrum. Reprinted with permission from Wastl *et al.*, ACS Nano **8**, 5233 (2014) [10]. Copyright 2014 American Chemical Society.

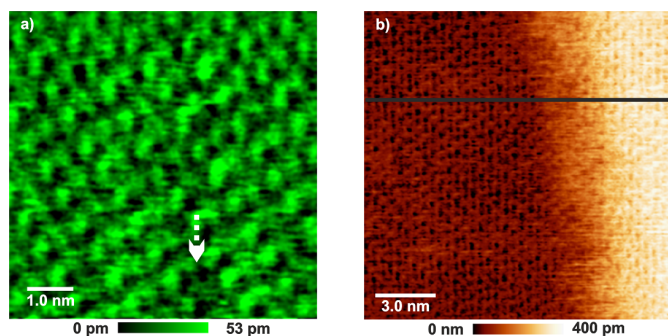


FIG. 6. Measurements on calcite. (a) Observation of a single atomic defect, indicated by the white arrow. (b) A single atomic step is shown, with atomic resolution on both terraces. Reprinted (adapted) with permission from Wastl *et al.*, ACS Nano **9**, 3858 (2015) [11]. Copyright 2015 American Chemical Society.

Our hypothesis for this is that the inert behavior of sapphire makes it hard to manipulate the tip apex. The Si tips were easier to manipulate but overall appeared much blunter. On top of this, the hydrophilic nature of silica meant that the tips were covered with water.

To summarize, we tested alternatives to the standard tungsten tips that we had been using. Both silicon and sapphire, due to their relatively low density, allowed us to create tips of the same size with greatly reduced mass, which is important for maintaining a high quality factor. The biggest difference between the two was in their hydrophobic and hydrophilic natures, which we could clearly see in $\Delta f(z)$ spectra.

V. OBSERVATION OF ATOMIC DEFECTS

The work discussed in this section was first reported in Ref. [11].

The reader might note that the magnitude of Δf when imaging surfaces in ambient conditions can be much greater than those when imaging in vacuum. Using a qPlus sensor with small amplitudes in vacuum, one expects frequency shifts from a few Hertz to a few tens of Hertz. In ambient conditions, we have observed atomic resolution with frequency shifts around hundreds of Hertz. The $\Delta f(z)$ spectra are also difficult to interpret, because of the additional forces at play: No longer can the observations be modeled with a combination of electrostatics, van der Waals interactions and chemical bonding. This begs the question: Are we sure that we are measuring the short-range interaction between the apex atom of the tip and the nearest surface atom? Or are we measuring a small area of the tip being pressed against the surface?

The most straightforward experimental proof that we are measuring a local interaction is to observe a local feature, such as a step edge or a single atom defect [1]. On graphene and graphite surfaces, a single atom defect is extremely unlikely, and the graphene sheet itself acts as a carpet over step edges. On the KBr surface, in larger area AFM images, we observed the step edges to be mobile. We therefore required surface whose steps would be clear and stationary and upon which we could find or create a single-atom defect.

Calcite (CaCO_3) is a common sample used in AFM

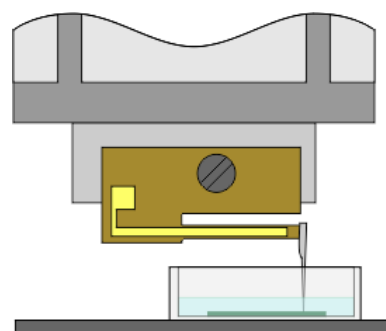


FIG. 7. Setup for the qPlus sensor to scan in a liquid environment. The sample is replaced with a bath that can support a liquid environment and the tip is longer to reach the sample surface.

experiments that is in abundant supply on the Earth. The $(10\bar{1}4)$ surface is a natural cleavage plane because of the weak out-of-plane bonds, leaving a surface whose unit cell includes two Ca atoms and two CO_3 groups. Moreover, calcite does not easily dissolve in water, meaning that the step edges are stationary and that atomic defects are stable.

Figure 6 shows both a step edge and a single atom defect that we have imaged on the calcite surface. In Fig. 6(a), the atoms can be seen on both terraces. The fringes at the step edge result from the long-range contributions, and have also been observed in AFM images taken in vacuum conditions [24].

VI. SUMMARY AND OUTLOOK

Our work has shown that the stiff qPlus sensor is sensitive to atomic features in ambient conditions. We observed atomic resolution in a range of different surfaces, single atomic defects, a step, and signatures of individual hydration layers.

Since the initial submission of this article, we have gone forward to realize atomic-scale imaging in a liquid environment. We built a small liquid cell and use a long tip to penetrate the liquid, sketched in Fig. 7. We also showed molecular resolution of a lipid bilayer in a liquid environment, which is experimental evidence that we can image with high spatial resolution and low contact force. [25]

However, there are still many ongoing challenges. How can we understand the $\Delta f(z)$ curve shown in Fig. 5(b)? And perhaps most excitingly, how can we achieve real atomic resolution of a biological sample in its native environment? The answers to these questions will require both advancement of measurement technology as well as a better understanding of the tip-sample interaction.

ACKNOWLEDGMENTS

A. J. Weymouth would like to thank the Surface Science Society of Japan, especially Ken-ichi Fukui and Yukio Hasegawa. He would also like to thank IBM Research (Zurich), the Swiss Embassy in Japan and Ms. Rohrer, for their effort towards the Heinrich Rohrer Rising Star Medal.

-
- [1] G. Binnig, C. F. Quate, and C. Gerber, *Phys. Rev. Lett.* **56**, 930 (1986).
- [2] Y. F. Dufrêne, T. Ando, R. Garcia, D. Alsteens, D. Martinez-Martin, A. Engel, C. Gerber, and D. J. Müller, *Nat. Nanotechnol.* **12**, 295 (2017).
- [3] F. Ohnesorge and G. Binnig, *Science* **260**, 1451 (1993).
- [4] T. Fukuma, K. Kobayashi, K. Matsushige, and H. Yamada, *Appl. Phys. Lett.* **87**, 034101 (2005).
- [5] F. J. Giessibl, *Appl. Phys. Lett.* **73**, 3956 (1999).
- [6] L. Gross, F. Mohn, N. Moll, P. Liljeroth, and G. Meyer, *Science* **325**, 1110 (2009).
- [7] M. Emmrich, F. Huber, F. Pielmeier, J. Welker, T. Hofmann, M. Schneiderbauer, D. Meuer, S. Polesya, S. Mankovsky, D. Kodderitzsch, H. Ebert, and F. J. Giessibl, *Science* **348**, 308 (2015).
- [8] T. Ichii, M. Fujimura, M. Negami, K. Murase, and H. Sugimura, *Jpn. J. Appl. Phys.* **51**, 08KB08 (2012).
- [9] D. S. Wastl, A. J. Weymouth, and F. J. Giessibl, *Phys. Rev. B* **87**, 245415 (2013).
- [10] D. S. Wastl, A. J. Weymouth, and F. J. Giessibl, *ACS Nano* **8**, 5233 (2014).
- [11] D. S. Wastl, M. Judmann, A. J. Weymouth, and F. J. Giessibl, *ACS Nano* **9**, 3858 (2015).
- [12] T. R. Albrecht, P. Grütter, D. Horne, and D. Rugar, *J. Appl. Phys.* **69**, 668 (1991).
- [13] F. Huber and F. J. Giessibl, *Rev. Sci. Instrum.* **88**, 073702 (2017).
- [14] E. Wutscher and F. J. Giessibl, *Rev. Sci. Instrum.* **82**, 093703 (2011).
- [15] D. Sedin and K. Rowlen, *Anal. Chem.* **72**, 2183 (2000).
- [16] M. Luna, F. Rieutord, N. A. Melman, Q. Dai, and M. Salmeron, *J. Phys. Chem. A* **102**, 6793 (1998).
- [17] F. J. Giessibl, *Rev. Mod. Phys.* **75**, 949 (2003).
- [18] F. J. Giessibl, in: *Noncontact Atomic Force Microscopy*, Vol. 2, edited by S. Morita, R. Wiesendanger, and F. J. Giessibl (Springer-Verlag, Berlin, Heidelberg, 2009) p. 121.
- [19] F. J. Giessibl, *Phys. Rev. B* **45**, 13815(R) (1992).
- [20] J. N. Israelachvili and R. M. Pashley, *Nature* **306**, 249 (1983).
- [21] R. C. Tung, T. Wutscher, D. Martinez-Martin, R. G. Reifenberger, F. Giessibl, and A. Raman, *J. Appl. Phys.* **107**, 104508 (2010).
- [22] E. V. Gorb, N. Hosoda, C. Miksch, and S. N. Gorb, *J. R. Soc. Interface* **7**, 1571 (2010).
- [23] F. Speck, J. Jobst, F. Fromm, M. Ostler, D. Waldmann, M. Hundhausen, H. B. Weber, and T. Seyller, *Appl. Phys. Lett.* **99**, 122106 (2011).
- [24] F. J. Giessibl and M. Reichling, *Nanotechnology* **16**, S118 (2005).
- [25] K. Puerckhauer, A. J. Weymouth, K. Pfeffer, L. Kullmann, E. Mulvihill, M. P. Krahn, D. J. Mueller, and F. J. Giessibl, *Sci. Rep.* **8**, 9330 (2018).